PERMEABILITY IMAGING FOR DETAILED RESERVOIR CHARACTERISATION

Lawrence T. Bourke
Reservoir Studies Group,
Schlumberger Exploration & Reservoir Services (UK) Ltd.,Aberdeen, UK.

Abstract High resolution permeability images generated by the nitrogen minipermeameter are a new approach to several key areas of sedimentological investigation. A study of sandstones derived from diverse depositional settings which visually appeared massive, have revealed heterogeneity on permeability images which can be identified as primary sedimentary fabric.

These images of permeability contrast frequently illustrate the subtle distribution of permeability reducing cements along preferential paths and provide improved visualisation of the progress of diagenesis through a reservoir fabric, (usually corresponding to primary depositional fabric). Minipermeameter imaging may therefore prove to be a valuable analytical tool for quantitative investigation of rock-fluid interaction. Permeability imaging effectively bridges the "scale gap" between microscopic investigation of diagenetic cement distribution and fluid flow modelling at the facies and reservoir zone scale.

This visual and quantifiable approach to assessing cement distribution could also provide a valuable additional technique in core

based investigation of rock mechanical properties in the laboratory.

The introduction of borehole imaging logs has meant that wireline vertical sampling rate (0.25cm) has outstripped typical conventional core vertical sampling intervals (25cm). Two-dimensional high resolution permeability images from core samples enable quantitative comparisons to be made with borehole wall images at similar sampling scales.

INTRODUCTION

The generation of high-resolution permeability images by fine grid sampling using a nitrogen minipermeameter on prepared sawcut core surfaces was first reported in Bourke *et al* (1990). This previous work demonstrated that minipermeameter images clearly have application in Petroleum Industry reservoir characterisation for the corroboration of ambiguous fabric revealed on microresistivity borehole wall images which are not visible in slabbed core samples. The technique involves the use of a minipermeameter with a probe tip having an internal diameter of 4mm or less. The probe minipermeameter was first described by Dykstra and Parsons (1950). Data gathered at a grid spacing of 4mm was found to be optimum for permeability image generation for direct comparison with borehole microresistivity images (Figure 2). The conclusions of this earlier paper were that permeability images could be used to verify borehole wall microresistivity images. Further, the latter had been shown to reveal subtle primary bedding textures not visually apparent on core samples but imaged on the borehole wall as microresistivity variations due to fluid saturation contrasts arising from subtle textural variations. The vertical resolution of these saturation textures on the borehole wall is in the order of 1 cm.

Since this initial work, the minipermeameter imaging technique has been applied in a variety of apparently featureless sands collected from surface and subsurface samples. This work revealed depositional fabric in all massive sands examined

suggesting that truly massive sandstones are apparently extremely uncommon. These visually massive sands were found to possess a diagenetic overprint on the primary depositional fabric. Such features are generally not revealed visually due to a lack of textural, colour or lithological contrast. The conclusions drawn from this work indicate that a number of applications exist for high resolution permeability imaging in conventional sedimentological analysis.

Approximately half of the data gathering for this work was acquired using a manual minipermeameter after the design of Clelland, (1986). The second half of the data gathering phase was achieved on the Statoil Automated Minipermeameter described in Halvorsen and Hurst, (1990).

IMAGE GENERATION

Selection of an appropriate probe tip diameter for minipermeameter imaging for the images presented in Bourke *et al*, (1990) was driven by the aim of matching minipermeameter resolution to that of the microresistivity images generated from the Formation MicroScanner Tool*. A 4mm internal diameter probe tip with a 4mm sampling grid used in approximately half of the data gathering for this work was found to be a appropriate (Figure 1). The Statoil Automated Minipermeameter small probe tip with an internal diameter of 3.5mm and sampled also at 4mm grid spacing was found to produce virtually identical results to those gathered at the same grid spacing with a 4mm probe. The use of successively smaller probe tips and increases in grid density will improve resolution of fine sedimentary detail as discussed in Hurst and Rosvoll (1990) but will reduce applicability in very coarse grained sandstones. While a decrease in sample grid length will tend to enhance image resolution, the possible benefits of high sampling rates must be considered practically in terms of

*Mark of Schlumberger

increasing the number of samples and hence scanning time. Successively larger probe diameters and increases in grid length rapidly reduce resolution of permeability images and increase the size threshold of features which can be imaged. Discernable reductions in image quality occur at 6mm grid spacing using a 4mm probe and marked deterioration in image quality was observed at 8mm grid spacing. Similarly increases in probe diameter reduce image quality significantly.

Image quality can also be compromised by defects on the sample surface. Irregular saw cuts if deep will influence probe tip sealing efficiency causing saw-cut artifact images. It has also been found that inconsistent sample surface cleaning can be seen on permeability images. A permeability anomaly can be created by filing a part of the surface of a sample due to irregular lodgement of rock fines in surface pore space. Surface cleaning is inevitably highly likely to modify permeability determined on the sample surface by nitrogen minipermeameter. If images are required only for semiquantitative applications then provided that surface preparation is consistent across the sample surface, image quality will not be compromised.

PERMEABILITY IMAGING, EXAMPLES

Three visually massive and featureless sandstones from three distinct depositional environments and one cross bedded sandstone were used to generate permeability images. The featureless sands also span a wide permeability range. Two of the massive sands were derived from quarries in the North East of Scotland and Northern England, the third from a North Sea well and the cross bedded sandstone from an outcrop exposure on the Moray Firth coast. The sandstones analysed, span three permeability ranges and include fine to medium grained sandstones. A high permeability, medium to coarse grained (3mm diameter) crossbedded sandstone was also imaged.

Example 1

Massive sandstone sampled from Clashach Quarry, Elgin Scotland: Hopeman Sandstone. The Hopeman sandstone is Permo-Triassic and comprises well silica cemented sands which are well sorted and include well rounded grains supporting an interpretation of aeolian dune deposition (Trewin *et al* (1987). The Hopeman sands are generally light brown and often reveal large scale cross bedding. The samples used in this study were chosen for their massive character. Grain size was consistently fine to medium (250-450 microns) and permeability range approximately 1.2-1.5 Darcies. Samples were cut from the quarry in an approximately vertical orientation forming three slabs totalling approximately 1 metre in length and 10.5 cm in width. Three permeability image "windows" were acquired over areas of the slab measuring 64 x 104 mm as illustrated in Figure 3. The grid of samples in each of these windows at a sample increment of 4mm was therefore 16 x 26 measurements. The images derived from these slabs are seen in Figure 4, where slightly inclined planar lamination can be clearly seen though completely lacking in the corresponding core photographs.

Example 2

Massive sandstone sampled from Birchover Quarry, England: Millstone Grit, Derbyshire. The Millstone grits in this locality are Namurian in age and are part of the Carboniferous measures in this area. The Birchover Quarry example was deposited in a fluvio-deltaic setting. The sands used for minipermeameter imaging were chosen for their apparent lack of primary bedding fabric. The sands are light brown in colour, well sorted with medium grain size (300 -350 microns). Petrographically these sands include ubiquitous quartz syntaxial overgrowths and abundant pore filling authigenic kaolinite. Shade variations in the lowest slab illustrated in Figure 5 appear to reflect slight differences in clay diagenesis, and a subtle change in sandstone texture was apparent in this zone.

The permeability range for these slabs is 200 - 800 millidarcies. The subtle variations in grain size and associated pore filling clay distribution have given rise to nitrogen flow rate variations seen on a vertical permeability traverse by minipermeameter over the three slabs. These permeability variations are illustrated in Figure 6 together with the indicated positions of minipermeameter windows in each slab. Here again, sands which display no visual evidence of primary bedding and only subtle grain size and diagenetic variations upon petrographic investigation clearly reveal primary bedding texture on permeability images, Figure 5.

Example 3

Massive sandstone from a Mesozoic North Sea reservoir. These sands comprise fine to medium grained, moderately well sorted sands deposited in a submarine gravity flow sequence. Permeability in the core samples analysed range from 80 - 750 millidarcies. A Formation MicroScanner Tool* (FMS) borehole imaging tool was run over these visually massive sands yielding mottled or vaguely bedded microresistivity images. The acquisition and processing of borehole microresistivity images by FMS is described in Lloyd *et al* (1986). Minipermeameter imaging was employed to establish whether borehole wall microresistivity imaging had revealed genuine reservoir fabric. The samples analysed were oil stained. Permeability imaging was carried out on samples before and after sohxlet refluxing with toluene to remove residual hydrocarbons. While permeabilities increased after cleaning, image character was not noticeable altered. This observation was also made by Clelland, 1984 in relation to minipermeameter measurement in uncleaned and cleaned core samples. Examples of minipermeameter and microresistivity images generated from these sands were reported in Bourke *et al*, 1990 and Adams *et al*, 1990 and are displayed in Figure 2. Permeability imaging has confirmed the presence of primary bedding fabric which was not visually apparent on core samples, and at the same time has provided confirmation that

the vaguely bedded and mottled features highlighted on borehole wall microresistivity images are genuine. The vertical and lateral sampling increment of the FMS tool are 0.1 inch (0.25 cm.) which gives an image resolution for resistive features of 1 cm. while conductive features of lesser dimensions may be revealed (Harker et al, 1990). Figure 2 illustrates the similarity in bedding resolution between microresistivity and permeability images.

Example 4

Cross bedded sandstone sampled from sea cliff outcrops at Burghead, Scotland: Burghead Beds. The Burghead beds are Triassic fluviatile sandstones with highly variable grain size and cementation characteristics, Trewin *et al*, 1987. This sample was chosen in contrast to the massive sands to provide distinctly visible primary bedding characteristics and an obvious diagenetic overprint. The upper two thirds of the sample are course to granule grade sands with permeabilities in the range of 2-3 Darcies. The lower third of the sample comprises medium to course grained sands with a marked quartz grain overgrowth region which cuts across primary bedding. Permeability in this zone is reduced to 300 - 450 millidarcies. In this instance, rather than producing a sawcut slab from the outcrop sample, a 3.25 inch (8 cm.) core was cut from the middle of the sample block, Figure 7. The Statoil Automated Minipermeameter was modified with the addition of a whole core jig (Figure 8) to accept a cylindrical sample. The derived permeability grid was otherwise generated as in the previous examples with a 4mm sample spacing. The permeability images derived from the outer surface of this sample accurately reveal cross bedding (Figure 9). Individual laminae are not necessary imaged where they are thinner than the width of the probe tip seal, however the general crossbedding texture including bedding discordancies have been reproduced. Additionally, the diagenetic variations which cross cut the primary bedding fabric have also been recognised.

SEDIMENTOLOGICAL APPLICATIONS

It is clear from the examples outlined in the previous section that high resolution permeability imaging by nitrogen minipermeameter is highly applicable for the definition of primary bedding fabric which is not visually apparent. This technique is not appropriate for use in the field, however in the laboratory it has significant advantages relative to core X-ray techniques in clean apparently massive sandstones. A core represents an extremely limited sample of a reservoir, cost effective techniques which reveal depositional information not otherwise apparent have value. Definition of specific primary bedding characteristics by permeability imaging could provide significant insight into the recognition of an appropriate depositional model in a field development.

A particularly promising application for permeability imaging is the unique perspective the technique offers in the recognition of cement distribution and its relationship to primary bedding. The use of petrographic data as a quantitative input to reservoir modelling and calibration of petrophysical computations is frequently inaccurate. This is due in part to poor interaction between geological and petrophysical disciplines but it is also attributable to the problem of scaling. The thin section investigates mineralogy and diagenesis at an intergranular level over an area of roughly 1.25 cm^2, the results of thin section point analyses are applied to wireline log data acquired from rock volumes of several m^3. Thin section petrographic analysis is also an extremely operator dependant practice. Minipermeameter images can provide a scale bridge in such situations. Consider the subtle cementation variations seen on permeability images in Figures 3 and 4. These diagenetic variations are concentrated on bedding planes which in this case give rise to permeability variance of 15% between light and dark beds in a sandstone with an average permeability of 1.35 Darcies. These light and dark laminae are approximately 1 cm. in width. At the scale of a thin section, it is unlikely that the

most skilled petrographer would be able to identify such subtle cementation variation in the scale of a thin section (particularly where there are no visible beds apparent at the macroscopic scale to guide his investigations) and would not be able to rationalise such variations to an organised rock fabric as has been demonstrated by permeability imaging.

In addition to providing a useful link in bridging scale differences, such images also provide insight into the advance of diagenesis within a relatively homogeneous sand body. In Figure 10, variations in average permeability between the upper middle and lower slabs can be quickly confirmed by variations in the connectivity of cemented regions. In the uppermost permeable slab the cemented zones are confined to alternate laminae which themselves are occasionally discontinuous. In the better cemented middle and lower slabs, the cemented regions have advanced into the intervening laminae as lobes or connecting fingers. Clearly the first case in Figure 10 will have a more pronounced permeability anisotropy than in the latter examples. The detailed definition of cement distribution defined quantitatively as permeability or nitrogen flow rate provides not only a new approach to numerical reservoir description but also could improve input parameters for rock properties modelling. The derivation of rock mechanical properties from wireline logs are based on the bulk log response for a certain rock volume measured by the various tools. Potentially, an awareness of the typical cement distribution in a rock body could have an important effect on the mechanical strength of a rock. Consider the sandstone example of figure 10 where a honeycomb of well cemented regions surround or partially surround beds or discontinuous zones of moderately cemented sands. The wireline log response in this situation will not be representative of either case. Such information on cement distribution could influence the selection and orientation of rock compressibility samples.

Quantitative analysis of permeability images can be achieved using proprietary image analysis packages. The images presented in this paper were displayed on a Formation Image Examiner workstation

[1] as discussed in Boyeldieu and Jeffreys, (1988). The "image binarisation" option on this workstation provides a technique for measuring areas of specified regions. The interpreter can highlight the preferentially cemented beds on an image to define the percentage area of this category as shown in Figure 11.

CONCLUSIONS

The computation of permeability images from fine grid surveys using a probe minipermeameter provides an exciting new area of application for minipermeametry. Such images are now known to reveal sedimentary detail in apparently featureless sands furnishing significant clues for depositional characterisation. The sensitivity of the technique is such that it offers advantages over core X-radiography. Permeability images also offer a new investigative technique to compliment thin section petrography and mechanical properties analysis. The recent growth in commercially available image analysis software makes the quantitative analysis of permeability image data a practical and inexpensive technique.

*1 Mark of Schlumberger

ACKNOWLEDGEMENTS

Thanks to Robert McWilliam for assisting in the acquisition of minipermeameter data used in the preparation of this paper. The sandstone samples from Clashach and Birchover quarries were supplied by Schlumberger Cambridge Research from their Drilling Invasion Studies project. Grateful acknowledgement to Statoil for the kind loan of the Statoil Automated Minipermeameter.

REFERENCES

BOURKE, L.T. 1989, Recognizing artifact images of the Formation MicroScanner Tool, *SPWLA Thirtieth Annual Logging Symposium, June 11th-14th.*, Denver.

BOURKE, L.T., CORBIN, N., BUCK, S.G., AND HUDSON, G., 1990, Permeability images - a new approach to reservoir characterisation. In Advances in Reservoir Geology, (ed) Ashton, M. *Special Publication of the Geological Society of London. (in press).*

BOYELDIEU, C., and JEFFREYS, P., 1988, Formation MicroScanner: New Developments, *SPWLA Eleventh European Evaluation Symposium, Oslo,* September.

CLELLAND, W., 1984, Measurement and analysis of small scale permeability distribution in sandstones, *unpublished Ph.D. thesis Heriot-Watt University, Department of Petroleum Engineering.*

DYKSTRA, H. and PARSONS, R.L., 1950, The prediction of oil recovery by waterflood. In *Secondary recovery in the USA. American Petroleum Institute.*

HALVORSEN, C., HURST, A., 1990, Principles practice and applications of Laboratory minipermeametry. pp.521-549 in Advances in Core Evaluation, *Proceedings of the Ist.Society of Core Analysts European Core Analysis Symposium, London.* (ed) Worthington, P. F.,

HURST A., and ROSVOLL K.J., 1990. Permeability variations and their relationship to sedimentary structures.

TREWIN, N.H., B.C., KNELLER and C. GILLEN, eds. 1987, Excursion guide to the Geology of the Aberdeen area, Scottish Academic Press, Edinburgh.

LLOYD, P.M., DAHAN, C., HUTIN,R., 1986, Formation imaging with electrical scanning arrays. A new generation of dipmeter results., paper N, *Trans. of the Tenth European Formation Evaluation Symposium,* Aberdeen

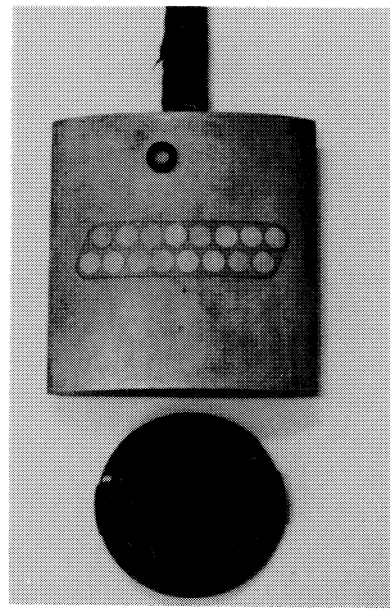

FIGURE 1 Comparison between the electrode size on a pad from a 4-pad FMS Tool and a 4mm "o" ring from the nitrogen minipermeameter used in this study (arrowed).

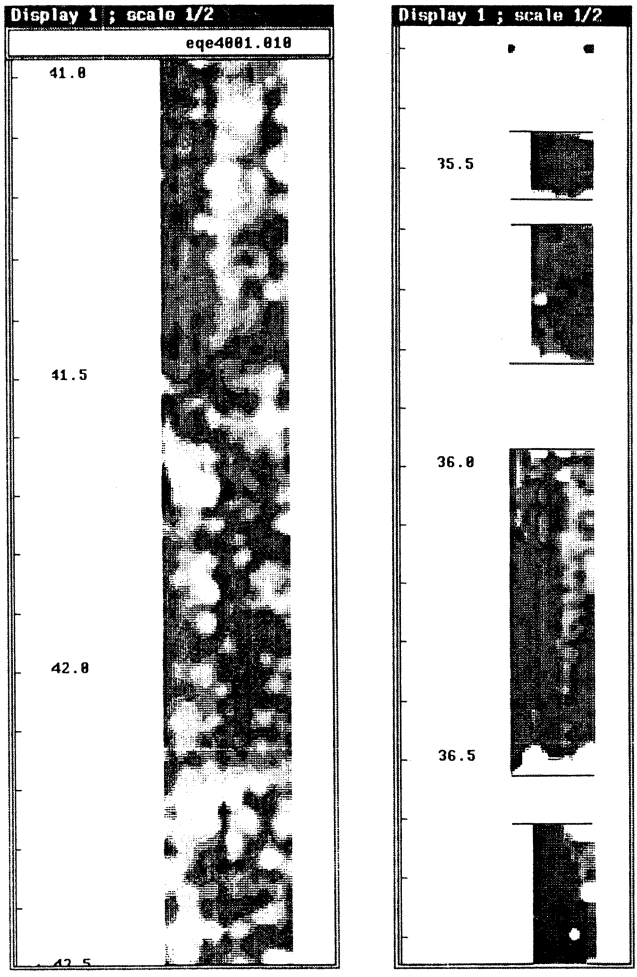

FIGURE 2 Comparison between Formation MicroScanner Tool microresistivity pad image (left) and minipermeameter images generated from core at the same depth (right) in massive sandstones. Extract from Bourke *et al* (1990).

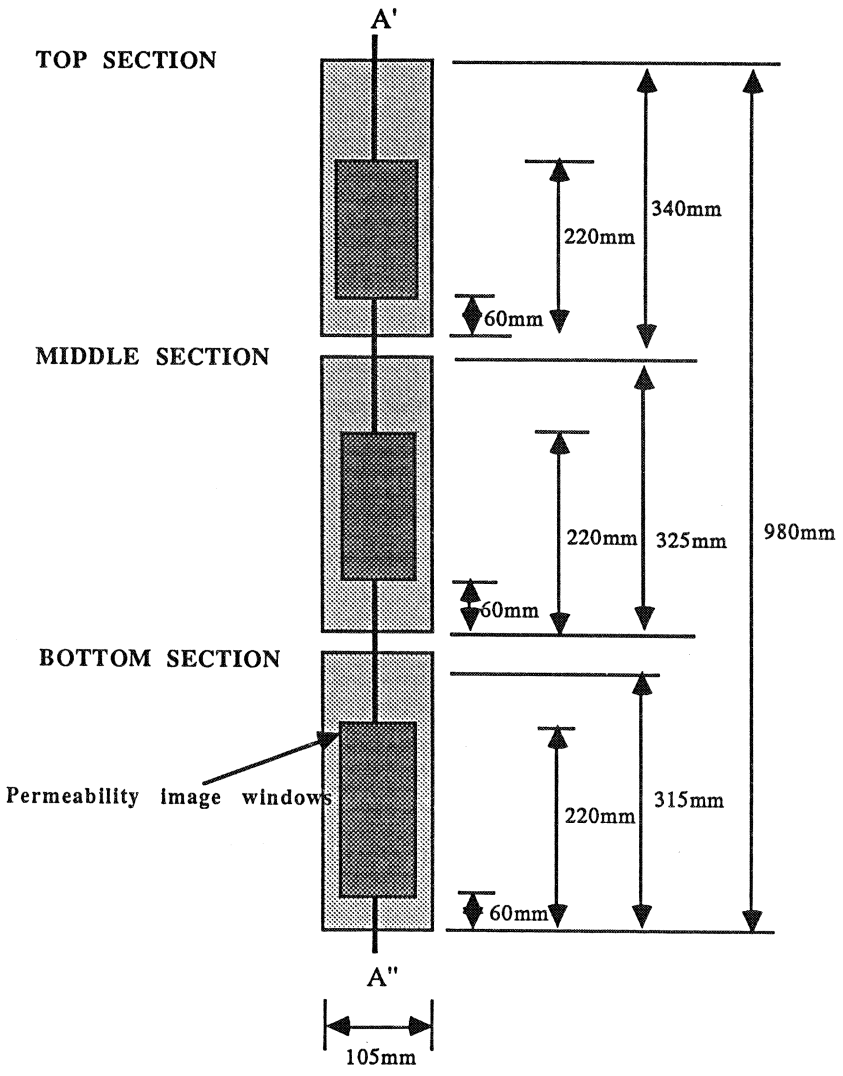

FIGURE 3 Schematic of permeability image positions on sandstone slabs (dark shaded) on Clashach Quarry samples.

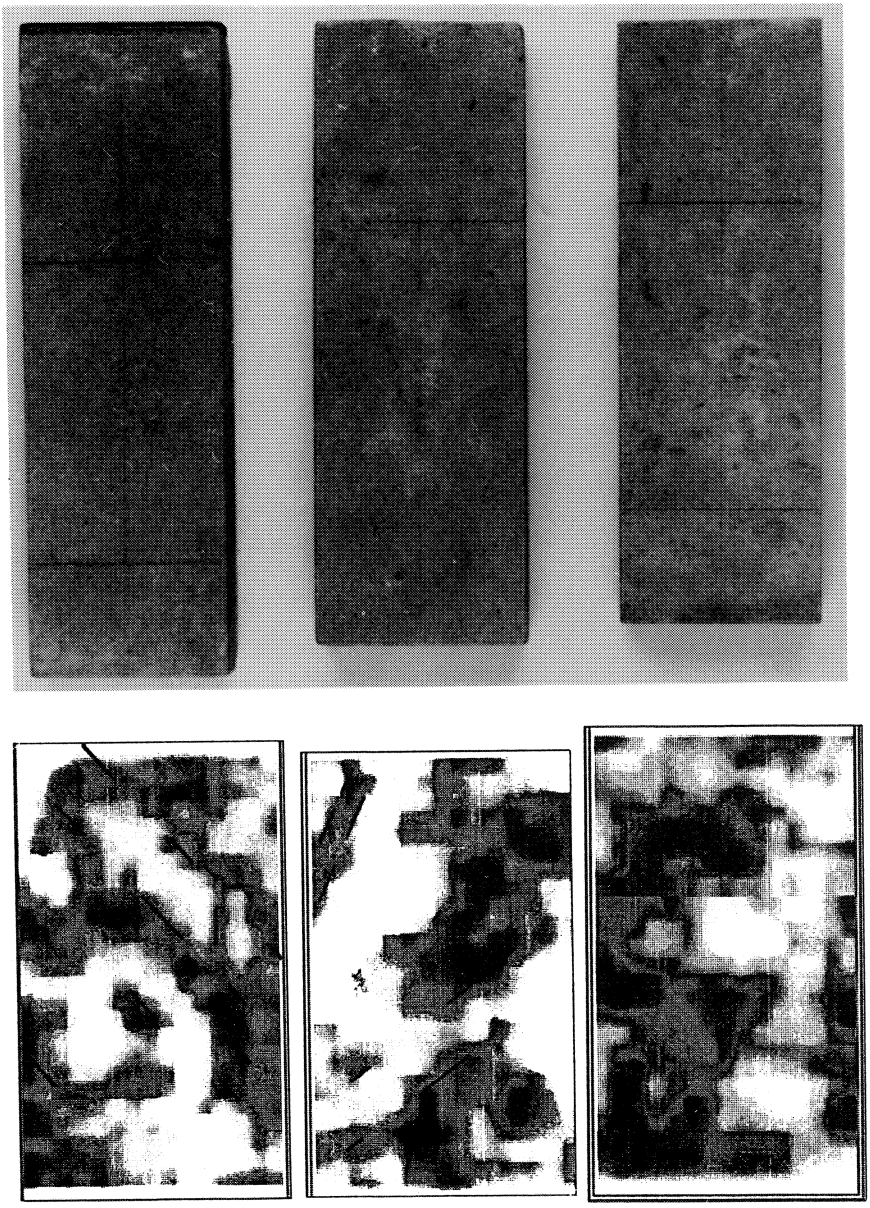

FIGURE 4 Photographs of Clashach Quarry massive sands (top sample left, bottom right). Corresponding permeability images revealing bedding are shown below. Bedding orientation is highlighted for convenience

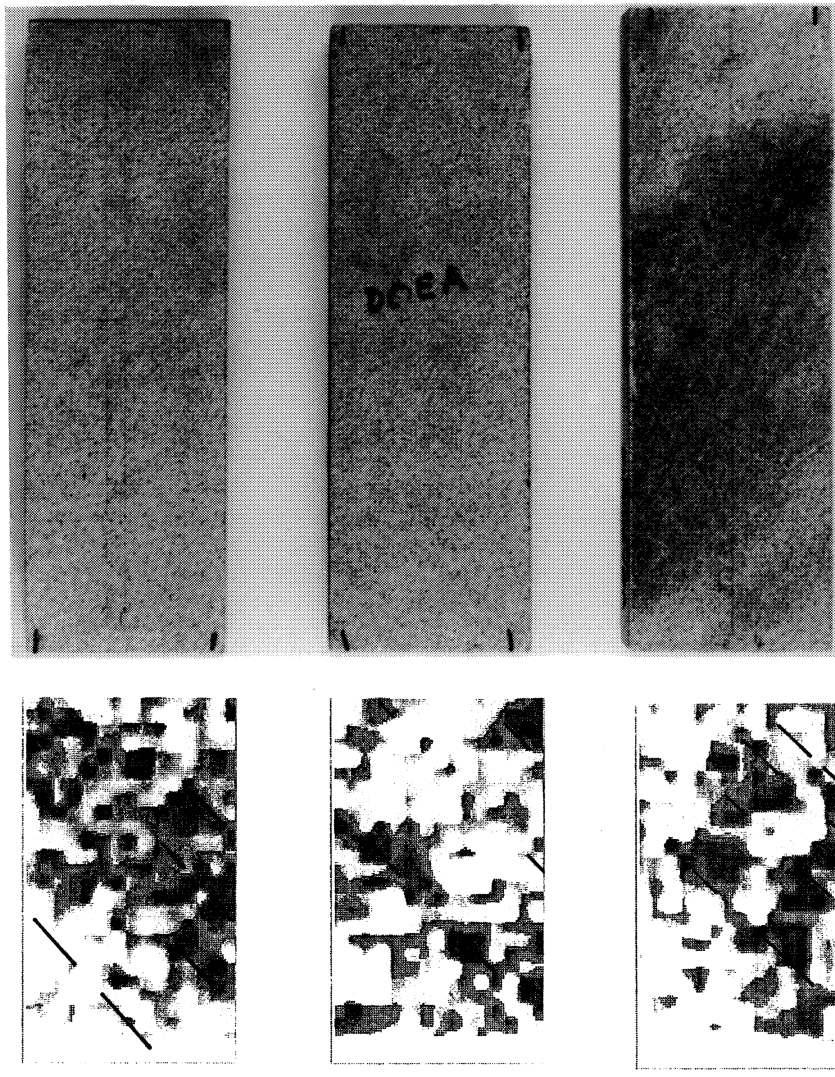

FIGURE 5 Photographs of massive sands fro Birchover Quarry and below, thei corresponding permeability images revealin bedding (highlighted).

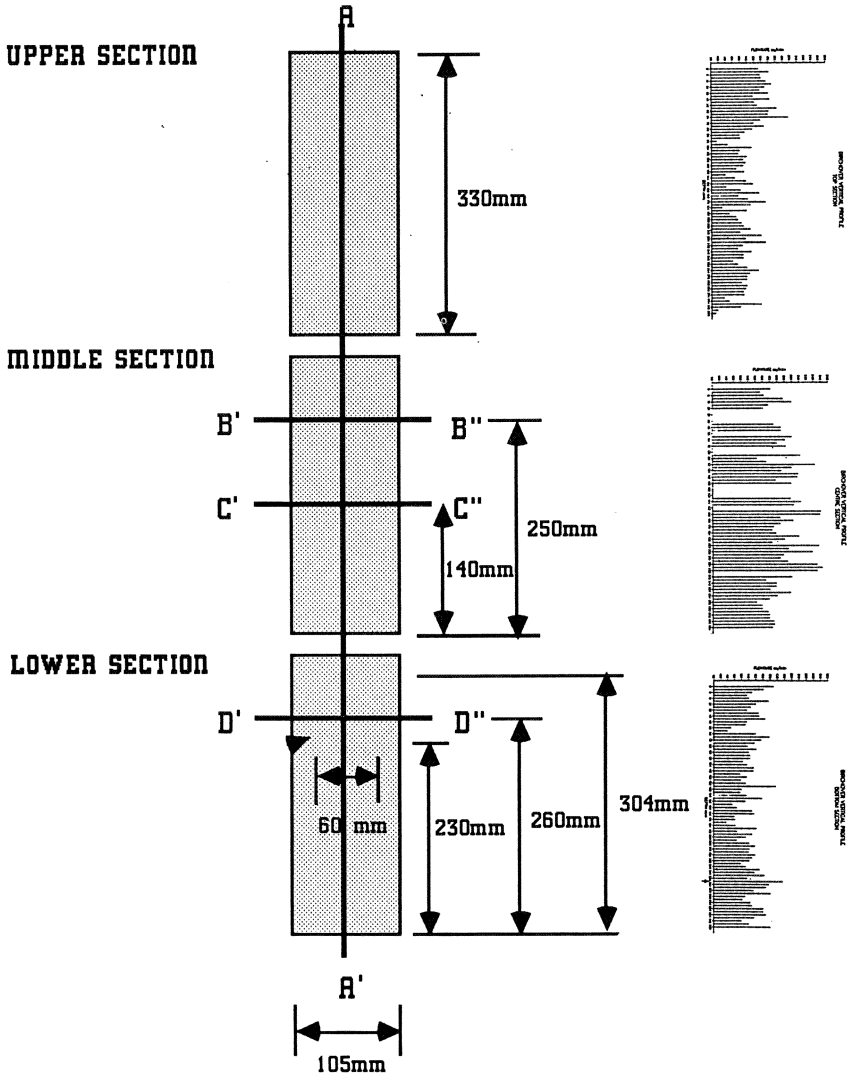

FIGURE 6 Schematic of Birchover Quarry sands and a single vertical minipermeameter tube flow rate profile in the section A-A'.

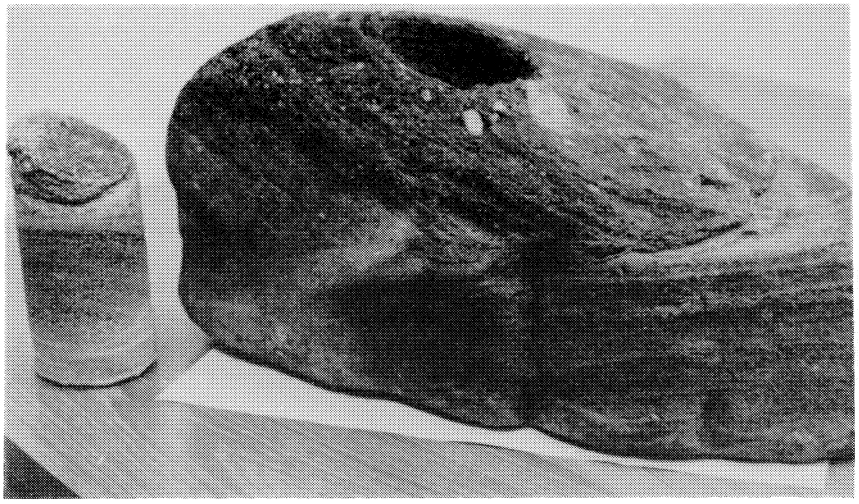

FIGURE 7 Fluvial crossbedded coarse sandstone sample from Burghead from which a 3,25 inch (8cm) core sample was cut. Sample is 23cm. high.

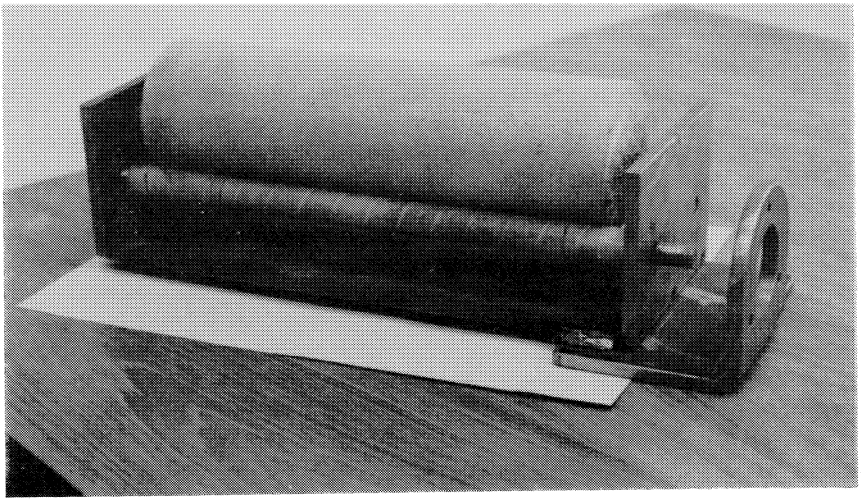

FIGURE 8 Whole core jig fabricated to accomodate core samples on the Statoil Automated Minipermeameter. Sample holder is 38cm. long.

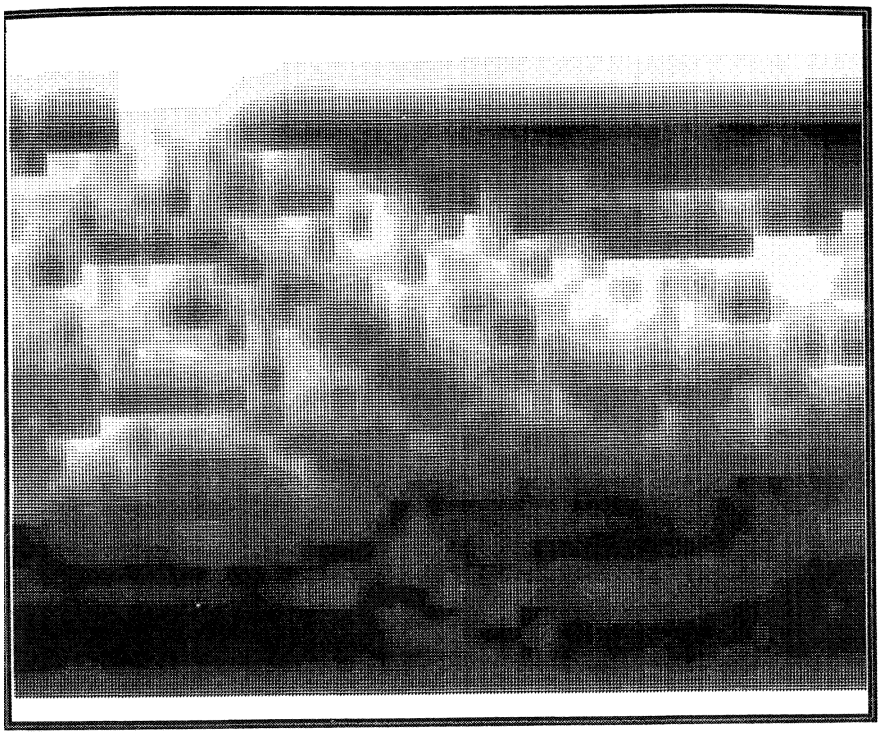

FIGURE 9 Unwrapped permeability image of crossbedded sandstone. The bottom quarter of the plot is partially cemented. Image scale is approximately 1:1. The dipping foresets from this crossbedded example describe sine curves in the unwrapped image. Bedding has good planarity.

TOP SECTION

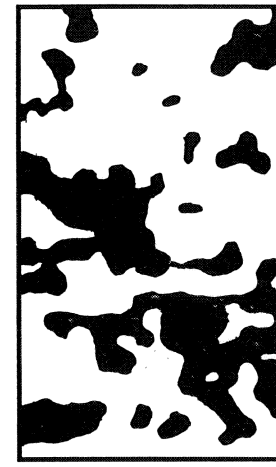

MIDDLE SECTION

BOTTOM SECTION

FIGURE 10 Preferentially cemented regions (black) from Fig. 5 demonstrating variations in degree of cementation relative to primary bedding (same orientation as for Figure 5).

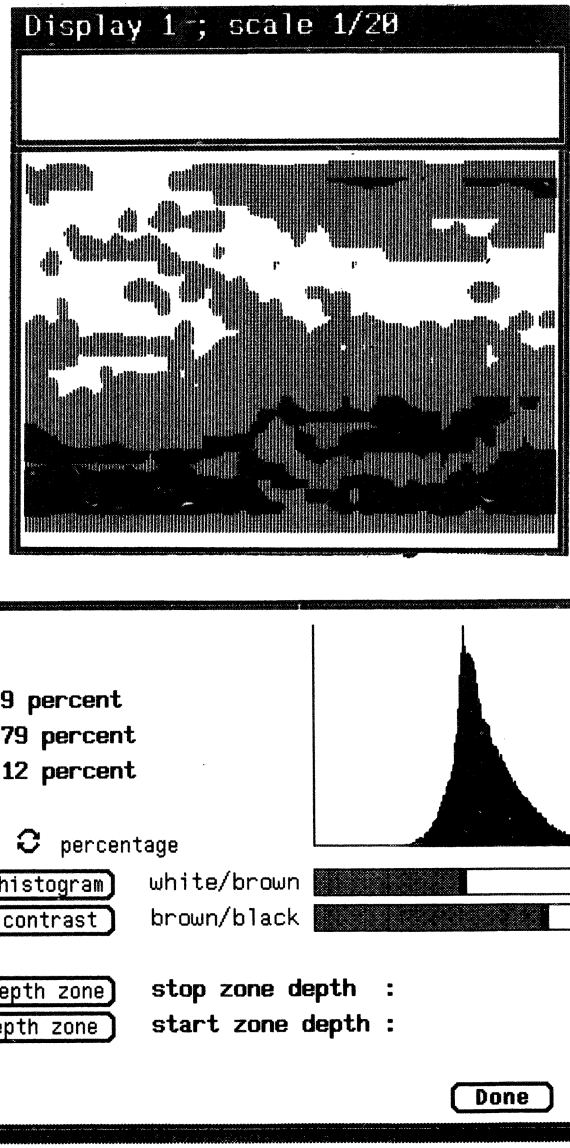

FIGURE 11 Image analysis workstation use for determination of areal percentages of selected regions.

Multi-phase Permeation Properties